# Kinetics and Computational Studies of an Aminosilane Reaction with a Silsesquioxane Silanol

**ARTICLE** *in* THE JOURNAL OF PHYSICAL CHEMISTRY A · JULY 2009

Impact Factor: 2.69 · DOI: 10.1021/jp9002998 · Source: PubMed



**5 AUTHORS**, INCLUDING:

Jonathan P Blitz
Eastern Illinois University
**67** PUBLICATIONS **1,066** CITATIONS
SEE PROFILE

Vlad Gun'ko
National Academy of Sciences of Ukraine
**209** PUBLICATIONS **2,993** CITATIONS
SEE PROFILE

# Kinetics and Computational Studies of an Aminosilane Reaction with a Silsesquioxane Silanol

**Reto Frei,[†] Jonathan P. Blitz,*[,†] Vladimir M. Gun'ko,[‡] Bradley E. Frost,[†] and Victor S. Sergeev[‡]**

*Department of Chemistry, Eastern Illinois University, Charleston, Illinois 61920, and Institute of Surface Chemistry, 17 General Naumov Street, 03164 Kiev, Ukraine*

*Received: January 12, 2009; Revised Manuscript Received: April 27, 2009*

The reaction between (3-aminopropyl)dimethylmethoxysilane (APDMS) with silica and silsesquioxane 3,5,7,9,11,13,15-heptacyclopentylpentacyclo[9.5.1.1$^{3,9}$.1$^{5,15}$.1$^{7,13}$]octasiloxan-1-ol was studied in hexane and tetrahydrofuran (THF) using experimental (reaction kinetics, FTIR) and quantum chemistry methods. In hexane at temperatures above 245 K, the reaction rate decreases with increasing temperature due to a reduction of prereaction complex formation at higher temperature. Below 245 K the reaction itself is rate limiting, resulting in a reaction rate decrease with decreasing temperature. The reaction occurs much faster in hexane than in THF in part because of stronger competitive effects of the O-containing polar solvent with the formation of APDMS/silsesquioxane prereaction complexes due to hydrogen bonding. Analysis of the experimental data and computational results suggest that the catalytic reaction is second-order with respect to APDMS, the second APDMS molecule plays the role of catalyst. Estimation of the activation energy using dynamic calculations give results much more in agreement with experiment than nondynamic calculations, since the limiting $H^+$ transfer stage occurs so quickly (~15 fs) that displacements of other atoms are insignificant to the activation energy.

## Introduction

(Aminopropyl)silanes are among the most widely used reagents for the surface modification of silica for a wide variety of applications such as composite materials,[1] chemical sensors,[2−4] metal ion adsorption,[5,6] new synthons for bionanotechnology as gene or drug transfer vehicles,[7] and bioseparations.[8] The technology for reacting the silica surface with (aminoproply)silanes has existed for some time, with a review by Vansant et al. detailing the important contributions of solid-state NMR and other methods.[9] It is known that aminosilanes exhibit uniquely enhanced reactivity compared to organosilanes with other functional groups.[10] This is assumed to be due to the fact that amines are known to be catalysts for the surface reaction of organosilanes with silica,[11−14] and therefore, the aminosilane contains its own catalyst.

Details of the kinetics and mechanism of the aminosilane surface modification reaction have not been investigated in much depth;[15−19] it is a complex problem. Industrially, these reactions are often done in aqueous solution, which provides the opportunity for hydrolysis and silane−silane condensation side reactions. To avoid such complications, many studies have utilized dry organic solvents as the reaction medium. With silica, which contains at least three different types of reactive surface hydroxyl groups (non-hydrogen-bonded, hydrogen-bonded, and diol), characterized by different accessibility in narrow and broad pores in silica gels, or in voids between nanoparticles of fumed silicas,[9] differentiating the reaction rate with each surface site is at best difficult.[20] It has also been suggested that the reaction of aminosilanes with silica is adsorption rate limited,[21] which makes interpretation of the kinetics problematic.

Soluble silsesquioxanes, which are partially condensed or with pendant silanols, have been used as model silica surfaces.[22−25] The use of silsesquioxanes to study the kinetics of these reactions possesses considerable advantages: (1) it is a soluble reaction system, thus eliminating the complications of the heterogeneous liquid/solid (or gas/solid) silica system; (2) a silsesquioxane of known structure can be chosen to contain one well-defined reactive group. Combining these advantages with the use of a monofunctional (aminoproply)silane in dry organic solvent (where a 1:1 (aminoproply)silane:silsesquioxane reaction is the only possibility), we obtain a reasonably well-defined system for the kinetic and mechanistic studies described in this report.

## Experimental Section

**Materials.** The silsesquioxane 3,5,7,9,11,13,15-heptacyclopentylpentacyclo[9.5.1.1$^{3,9}$.1$^{5,15}$.1$^{7,13}$]octasiloxan-1-ol (>95%, Aldrich), hexane (>99.9%, Fisher), Cab-O-Sil HS5 (Cabot Corp.), *o*-dichlorobenzene (Mallinckrodt), and *n*-butylamine (Aldrich, >99.5%) were used as received. Tetrahydrofuran (THF, Mallinckrodt, >99.8%) and (3-aminoproply)dimethylmethoxysilane (APDMS) (Silar Laboratories) were distilled in $N_2$ prior to use.

**Reactions.** Typically, 200 mg of silsesquioxane (0.22 mmol) was dissolved in either hexane or THF with 15.0 $\mu$L (0.13 mmol) of *o*-dichlorobenzene and 37.0 $\mu$L (0.22 mmol) of (3-aminopropyl)dimethylmethoxysilane in a 25.0 mL volumetric flask. The reactions were carried out in a constant temperature bath. Sample aliquots were taken at various time intervals and immediately analyzed for the extent of reaction by solution FTIR spectroscopy. Blank solution reactions were carried out in both solvents with 0.22 mmol of *n*-butylamine substituted for the aminosilane. Below room temperature reactions were carried out in dry ice slurry baths; above room temperature reactions were carried out using an immersion bath circulator.

Silica reactions were carried out with 0.500 g of Cab-O-Sil HS-5 by slurry with 10.0 mL of either hexane or THF in a 50

* To whom correspondence should be addressed. Phone: 217 581 6369. Fax: 217 581 6613. E-mail: jpblitz@eiu.edu.
[†] Eastern Illinois University.
[‡] Institute of Surface Chemistry.

10.1021/jp9002998 CCC: $40.75 
Published on Web 05/21/2009

mL conical flask. In a separate beaker 42.0 μL of (3-aminopropyl)dimethylmethoxysilane was dissolved in 10.0 mL of corresponding solvent. Upon mixing and swirling the contents for 15 s, the reaction was allowed to proceed for reaction times of 2, 5, 30, and 60 min (each a separate experiment). After the specified reaction time, the slurry was filtered, washed twice with 10 mL of hexane, and dried in vacuum at 110 °C for 90 min prior to analysis by transmission FTIR spectroscopy of the dried solid.

**FTIR Analysis.** All spectra were obtained with a Digilab FTS3000 FTIR spectrometer with DTGS detector. Typically 16 scans were coadded at 4 $cm^{-1}$ nominal resolution. Solution spectra were obtained using a 1.0 mm path length cell equipped with NaCl windows after spectral subtraction of the solvent (hexane or THF) using standard spectrometer software. In hexane, reaction progress was monitored by the integrated intensity of the silanol O−H stretching peak (3725−3700 $cm^{-1}$). In THF, reaction progress was monitored by the OH peak height at 3310 $cm^{-1}$, to avoid contributions from N−H stretching bands.

Solid silica samples were analyzed by placing a small amount of Cab-O-Sil between NaCl plates and rotating to produce a thin film. The relative non-hydrogen-bonded silanol concentration was obtained by integration of this peak (3752−3735 $cm^{-1}$) ratioed to a Si−O−Si combination band (1910−1825 $cm^{-1}$) used as an internal standard, in this case to correct for different amounts of silica in the IR beam.

**Computational Studies.** Quantum chemical calculations of interactions between silsesquioxane and APDMS were carried out for both gaseous and liquid media using the Gaussian 98[26] and 03,[27] GAMESS (version 24 March 2007 (R1)[28a] and PC version 7.15[28b]), and GAMESOL[29] program packages with ab initio (6-31G(d,p) and 6-31G(d) basis sets) and DFT (B3LYP/6-31G(d,p)) techniques. The transition states (TS) for various mechanisms were computed (using QST2, QST3, and EF options in Gaussian and DRC in GAMESS) assuming noncatalytic and intra- and interautocatalytic reactions. The APDMS amino group can play the role of catalyst affecting $H^+$ transfer between silsesquioxane SiOH and $SiOCH_3$ of APDMS. For simplicity, we substituted H for cyclopentyl groups on the silsesquioxane, and the second APDMS molecule in the interautocatalytic reaction was replaced by $NH_3$. Solvation effects were analyzed using the SM5.42R/6-31G(d) method[29] (hexane and tetrahydrofuran as solvents) and IEFPCM/B3LYP/6-31G(d,p)[26,27] (tetrahydrofuran and heptane instead of hexane) with the HF/6-31G(d,p) geometry.

## Results and Discussion

The reaction of (3-aminopropyl)dimethylmethoxysilane with the silsesquioxane is

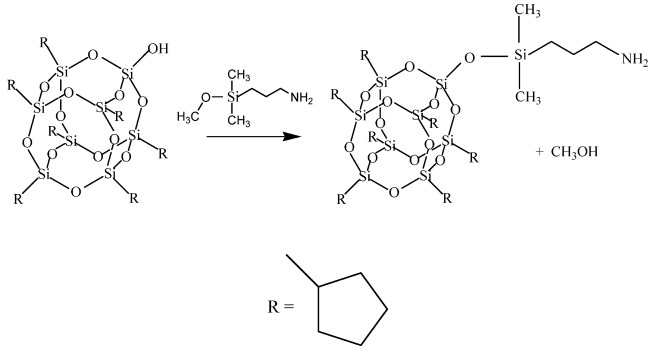


In Figure 1A representative FTIR spectra in the OH stretching region of the silsesquioxane reaction with the aminosilane in hexane

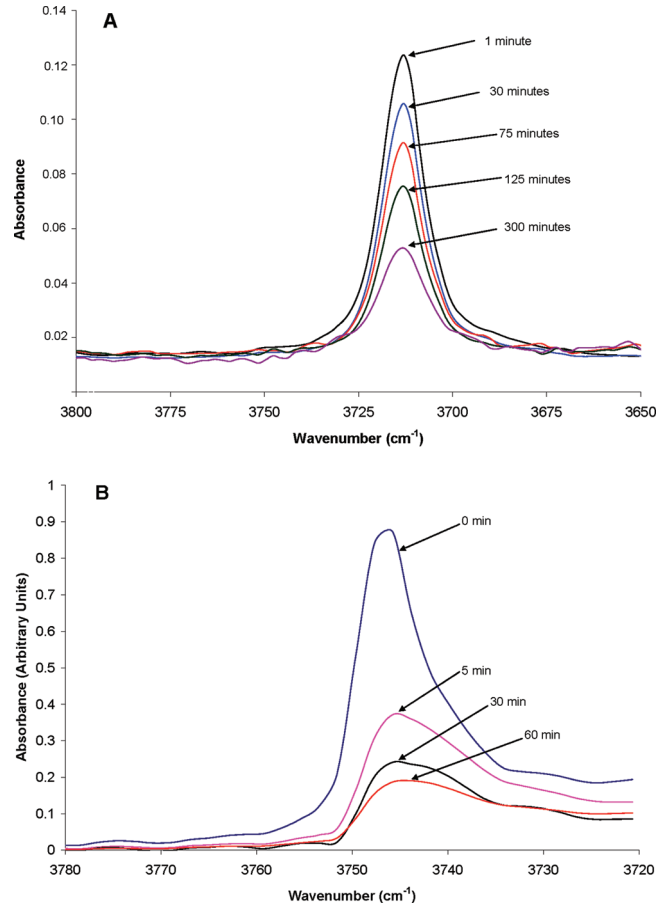


**Figure 1.** FTIR spectra showing the loss of silsesquioxane silanol in hexane (A) and silica surface silanol from THF slurry (B) after reaction with (3-aminopropyl)dimethylmethoxysilane as a function of time.

during the course of reaction are presented. Using the integrated OH band area as a quantitative monitor of reaction extent, plots of the concentration of unreacted silsesquioxane as a function of time in hexane and THF can be obtained. In a similar fashion, the extent of non-hydrogen-bonded silanol content can be measured on silica during the course of reaction from THF or hexane slurry (Figure 1B).

Figure 2 contains plots of the concentration of unreacted silsesquioxane (A) and silica non-hydrogen-bonded silanols (B) as a function of time at 25 °C. The data clearly show a pronounced solvent effect; the rate of reaction for both the silsesquioxane and silica silanols is greatly reduced in THF compared to hexane. Since the reaction of (3-aminopropyl)dimethylmethoxysilane with silica is so fast (particularly in hexane) as to be adsorption rate limited, and detailed kinetic investigations with silica are extremely complex as previously discussed, further experimental studies focused on the kinetics of the silsesquioxane reaction in hexane solution.

A series of 1:1 aminosilane reactions with silsesquioxane in hexane solution were completed at various temperatures. The time required for the reaction to reach 50% completion was estimated using plots similar to that shown in Figure 2. Table 1 provides $t_{1/2}$ values as a function of temperature. While it is expected that as the temperature is increased $t_{1/2}$ would decrease as a result of a reaction rate increase, this general trend is reversed at temperatures of −30 °C and above. There is an inflection point in the data, both above and below which the reaction rate decreases ($t_{1/2}$ increases), indicating that there are two regimes where the reaction rate is dictated by different processes.

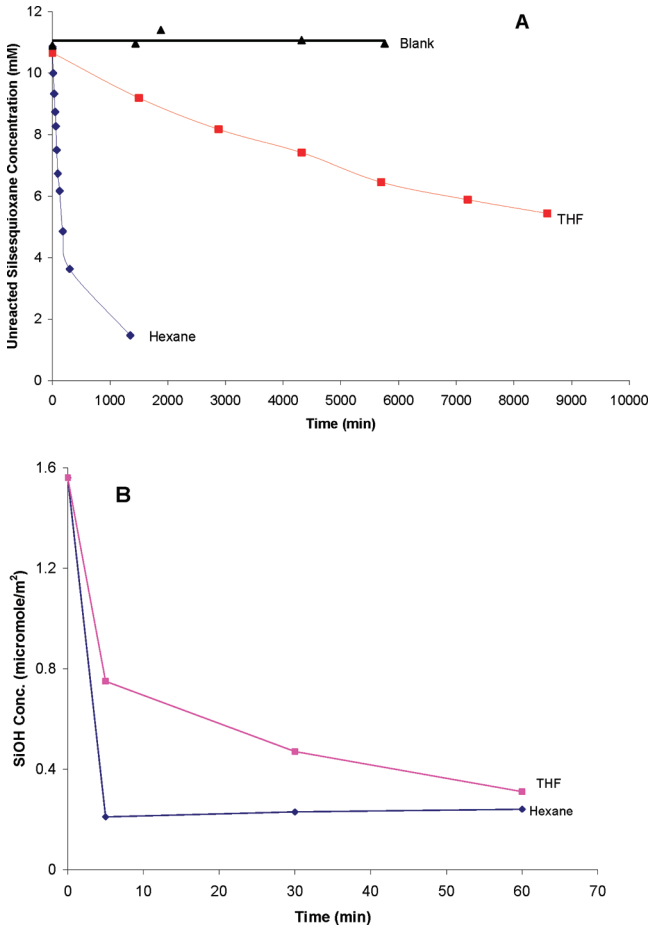


**Figure 2.** Concentration of unreacted silsesquioxane (A) and unreacted non-hydrogen-bonded silica silanol (B) after reaction with (3-aminopropyl)dimethylmethoxysilane as a function of time.

**TABLE 1: Estimates of Reaction $t_{1/2}$ Data as a Function of Temperature for the Reaction of (3-Aminopropyl)dimethylmethoxysilane in Hexane with the Silsesquioxane**

| temp (°C) | $t_{1/2}$ (min) |
|---|---|
| 20 | 165 |
| 15 | 115 |
| 0 | 60 |
| −15 | 45 |
| −30 | 35 |
| −45 | 70 |
| −53 | 90 |
| −60 | 180 |
| −78 | 1520 |

The reaction mechanism can be envisioned as a two-step process; the first being a fast equilibrium formation of a prereaction complex (pre-equilibrium), the second step chemical reaction. Without implying any molecularity to the reaction mechanism, the reaction can be simply and qualitatively depicted as follows:

$$\mathrm{A} + \mathrm{B} \underset{k_1}{\overset{k_1}{\rightleftharpoons}} \mathrm{A{-}{-}{-}B} \qquad (1)$$

$$\mathrm{A{-}{-}{-}B} \xrightarrow{k_2} \mathrm{C} \qquad (2a)$$

Assuming at higher temperatures the concentration of the prereaction complex as depicted in eq 1 is rate limiting, the reaction

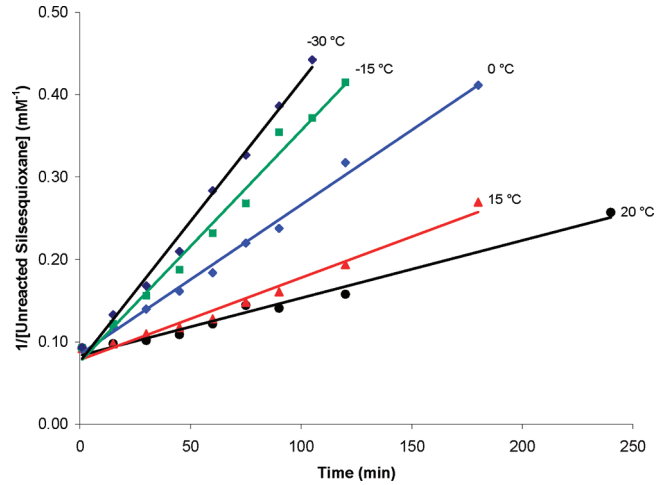


**Figure 3.** Relative reaction rates of silsesquioxane silanol with (3-aminopropyl)dimethylmethoxysilane at various temperatures using the second-order integrated rate expression.

measured by silsesquioxane loss, as accomplished experimentally, would exhibit overall second-order kinetics. If the rate of $k_2$ is much less than the rates responsible for the pre-equilibrium, then the second reaction does not affect the prereaction complex concentration (A···B), and this complex is in a steady state. Defining [A] as the aminosilane concentration, [B] as the silsesquioxane concentration, [C] as the product concentration, and $K$ as the equilibrium constant of the pre-equilibrium step, the following argument can be developed:[30]

$$\mathrm{d[A{\cdots}B]}/\mathrm{d}t = k_1[\mathrm{A}][\mathrm{B}] - k_{-1}[\mathrm{A{\cdots}B}]$$

$$k_1[\mathrm{A}][\mathrm{B}] - k_{-1}[\mathrm{A{\cdots}B}] = 0$$

$$[\mathrm{A{\cdots}B}] = k_1/k_{-1}[\mathrm{A}][\mathrm{B}] = K[\mathrm{A}][\mathrm{B}]$$

$$\mathrm{d[C]}/\mathrm{d}t = -\mathrm{d[A{\cdots}B]}/\mathrm{d}t = k_2K[\mathrm{A}][\mathrm{B}] \qquad (3)$$

With this scheme, a decrease in reaction rate at higher temperatures (−30 °C and above) is the result of a decrease in the concentration of the prereaction complex (i.e., a decreased $K$). Although the rate constant $k_2$ probably increases with temperature, the decreasing equilibrium constant value can cause the product $k_2K$ to decrease, thus causing the measured reaction rate to decrease. A decrease in the equilibrium constant with increased temperature for process 1 is expected. The adsorption of amines onto silica surface silanols is an exothermic process,[31] and this first step almost certainly involves complex formation of an aminosilane with the silsesquixane silanol. A decrease in reaction rate with increasing temperature has been observed for amine catalyzed silica silylation reactions, the data being qualitatively rationalized in a similar fashion.[32]

Figure 3 contains plots using the overall second-order integrated rate expression for reactions at temperatures ranging from −30 to +20 °C. The $R^2$ correlation coefficients to the linear least-squares fits are all greater than 0.98. These good fits to second-order kinetics are not surprising; however this provides no information on the kinetics and mechanism of the reaction depicted in step 2 separate from the pre-equilibrium step.

At temperatures of −45 °C and below, the reaction is not limited by the concentration of prereaction complex, but by step 2 in Scheme 1: that of reaction to form the aminosilane-modified silsesquioxane product. At least two general scenarios can be

**SCHEME 1**

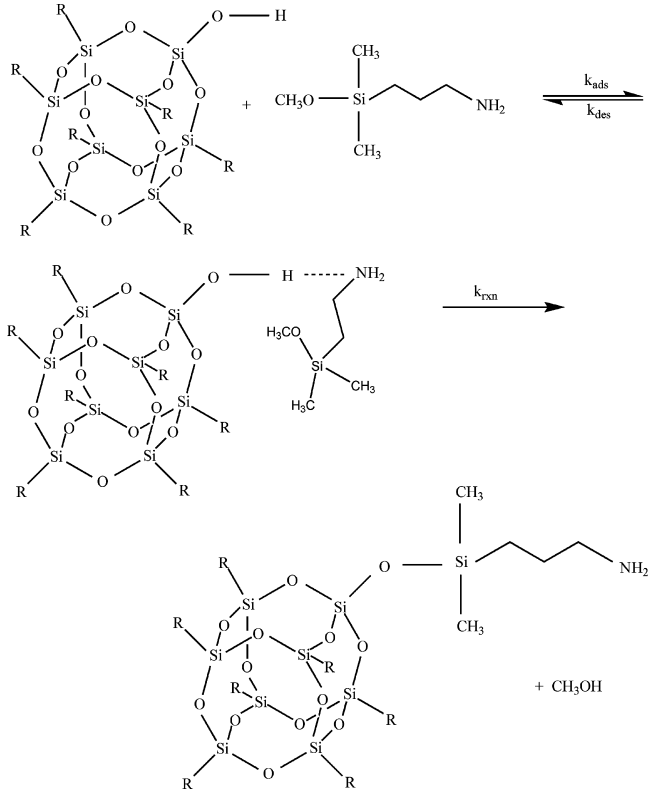


postulated for the reaction in step 2. In either case an amine is thought to be involved to catalyze the reaction, which explains the unusually high reactivity of aminosilanes. One is the prereaction complex reacts directly to form products. This involves catalysis with the amine in the aminosilane that is in the prereaction complex, an intramolecular amine catalysis reaction as qualitatively illustrated in Figure 4A and more symbolically in Scheme 1, eq 2a. The second possibility is that the prereaction complex formed in step 1 is catalyzed to form products by a second aminosilane, depicted in Figure 4B and eq 2b below.

$$A + A\text{---}B \rightarrow C + A \qquad (2b)$$

It should be theoretically possible to differentiate the reaction paths depicted by eqs 2a and 2b. If the rate of reaction is dictated by the process shown in eq 2a, then it can be shown that the rate of reaction is identical to that shown in eq 3; i.e., first-order with respect to APDMS (overall second-order). If the reaction rate is dictated by the process depicted in eq 2b, then the reaction rate is second-order with respect to APDMS, as depicted in eq 4 (overall third-order):

$$d[C]/dt = -d[A\cdots B]/dt = k_2 K[A]^2[B] \qquad (4)$$

All reactions discussed thus far were performed with a silsesquioxane to aminosilane stoichiometric ratio of 1:1. A comparison of overall second- and third-order fits to these low temperature data is inconclusive, providing no insight into the molecularity of the reaction step.

Assuming that the APDMS/silsesquioxane reaction obeys the Arrhenius law, the distribution function ($f(E)$) of the activation energy of the reaction in hexane can be calculated using the

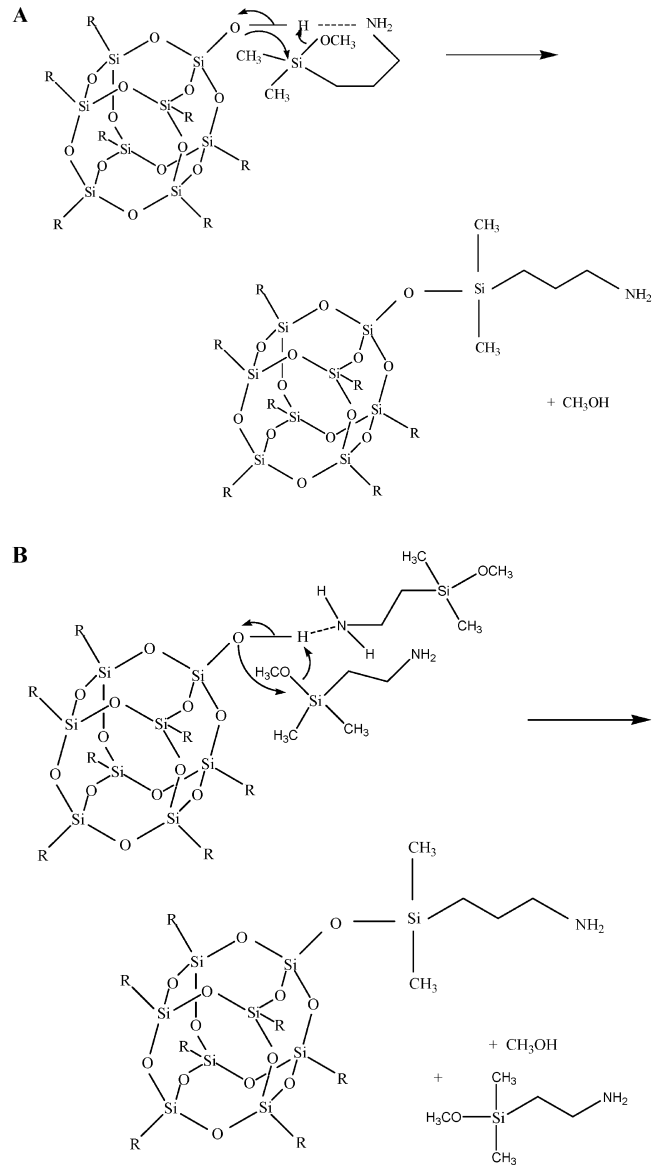


**Figure 4.** Intramolecular amine catalysis of reaction (A) and amine catalyzed silylation with two amines in the transition state (B).

temperature dependence of the relative amount of reacted silsesquioxane ($a_r = (C_{SS,0} - C_{SS})/C_{SS,0}$, where $C_{SS,0}$ and $C_{SS}(t,T)$ are the initial and residual amounts of silsesquioxane, respectively) at $T < 245$ K and $t = 1$ h (Figure 5a). These calculations were solved with the corresponding integral equation with a regularization procedure based on the CONTIN algorithm[33]

$$a_r(t,T) = \int_{E_{min}}^{E_{max}} k_0(t)\, f(E) \exp\left(-\frac{E}{RT}\right) dE \qquad (5)$$

where $k_0(t)$ is the pre-exponential factor depending on reaction time and the $C_{SS,0}$ value, $R$ is the gas constant, and $E_{min}$ and $E_{max}$ are the minimal and maximal $E$ values on integration. The first moment of $f(E)$ calculated as $\langle E\rangle = (\int_{E_{min}}^{E_{max}} E f(E)\, dE)/(\int_{E_{min}}^{E_{max}} f(E)\, dE)$ is equal to 50.5 kJ/mol, which is close to the average value of the effective activation energy (45 kJ/mol) from the kinetic data (Figure 5c).

A set of experiments was performed in the low temperature regime (−60 °C), where the reaction is considered to be reaction rate limited, by varying the silsesquioxane to aminosilane stoichiometric ratio. These data were fit to second- and third-

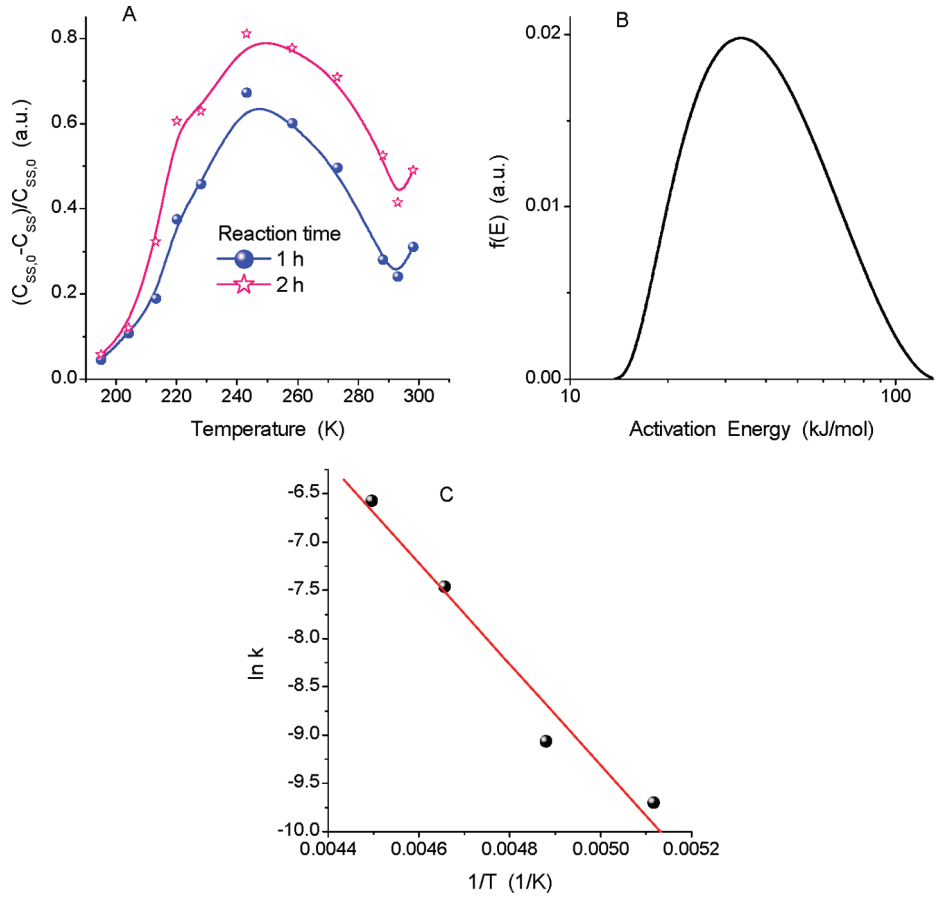


**Figure 5.** (A) Relative amount of reacted silsesquioxane as a function of reaction temperature at reaction time $t = 1$ and 2 h. (B) Distribution function of activation energy of reaction between silsesquioxane silanol and APDMS in hexane at $t = 1$ h and $T < 250$ K. (C) Arrhenius plot of data at $T < 250$ K.

**TABLE 2: Data from Reactions at −60 °C**

| aminosilane/ silsesquioxane mole ratio | 2nd-order $R^2$ | 3rd-order $R^2$ | $t_{1/2}$ (min) |
|---|---|---|---|
| 0.5/1 | 0.964 | 0.983 | 450 |
| 1/1 | 0.985 | 0.991 | 220 |
| 2/1 | 0.991 | 0.943 | 60 |
| 0.5/1 + 0.5 butylamine | 0.969 | 0.978 | 160 |

order integrated rate expressions, the $R^2$ linear least-squares correlation coefficients given in Table 2. One can see a general trend that as the aminosilane/silsesquioxane ratio increases, the fit to a second-order expression increases relative to the third-order fit. With increasing mole ratios of aminosilane to silsesquioxane, as the reaction proceeds, the relative concentration of aminosilane is less affected. This more closely resembles that of a reaction which is pseudo-first-order in aminosilane, thus the reaction better fits an overall second-order reaction under these conditions. On the other hand, when there is less than a stoichiometric amount of aminosilane, the data best fit overall third-order kinetics, indicating that the reaction exhibits at least some third-order character, with a contribution from a mechanism like that depicted by eq 2b and Figure 4b.

Additional evidence of two amine bearing molecules participating in the reaction can be seen in the $t_{1/2}$ data of Table 2. Two reactions were performed with an aminosilane/silsesquioxane ratio of 0.5/1; one contained no additional reagent, and the other contained a second 0.5 equiv of butylamine in addition to the 0.5 equiv of aminosilane. While the butylamine can participate in the reaction as a catalyst, it does not undergo reaction with the silsesquioxane. Addition of butylamine causes the $t_{1/2}$ value to decrease, indicating it is a participant in the rate limiting step of this reaction (i.e., eq 2b). Furthermore, the $t_{1/2}$ value obtained in the presence of 0.5 equiv of aminosilane + 0.5 equiv of butylamine, is very similar to the $t_{1/2}$ value found in the reaction with 1 equivalent of aminosilane. Thus the added butylamine is an effective substitute in the transition state for a second (aminoproply)silane. Taken together these experimental data strongly suggest that a third-order reaction mechanism is a likely contributor, and that at least one transition state consists of two aminosilanes and a silsesquioxane (silanol). Further modeling of the transition state and the overall reaction was done using computational methods.

To elucidate some aspects of the interactions between APDMS and silsesquioxane, the transition states (TS) were calculated for noncatalytic, intercatalytic (eq 2a, Figure 4B), intracatalytic (eq 2b, Figure 4A), and a THF catalyzed reaction (Figure 6). Transition-state calculations using the B3LYP/6-31G(d,p)//6-31G(d,p) basis set give smaller $E^{\neq}$ values, and a smaller difference between the noncatalytic and catalyzed reactions compared to equivalent HF calculations (Table 3). It can be seen that the reaction in vacuum is characterized by large $E^{\neq}$ values, even with consideration of the autocatalytic effect, compared to the experimental data in solution. This may be due in part to $H^+$ transfer under the additional action of a catalyst (modeled by $NH_3$ and THF here) without consideration of solvation effects. These effects were analyzed using calculations with the SM5.42R/6-31G(d)//6-31G(d,p)[29] and IEFPCM/B3LYP/6-31G(d,p)//6-31G(d,p)[26,27] methods (Table 3).

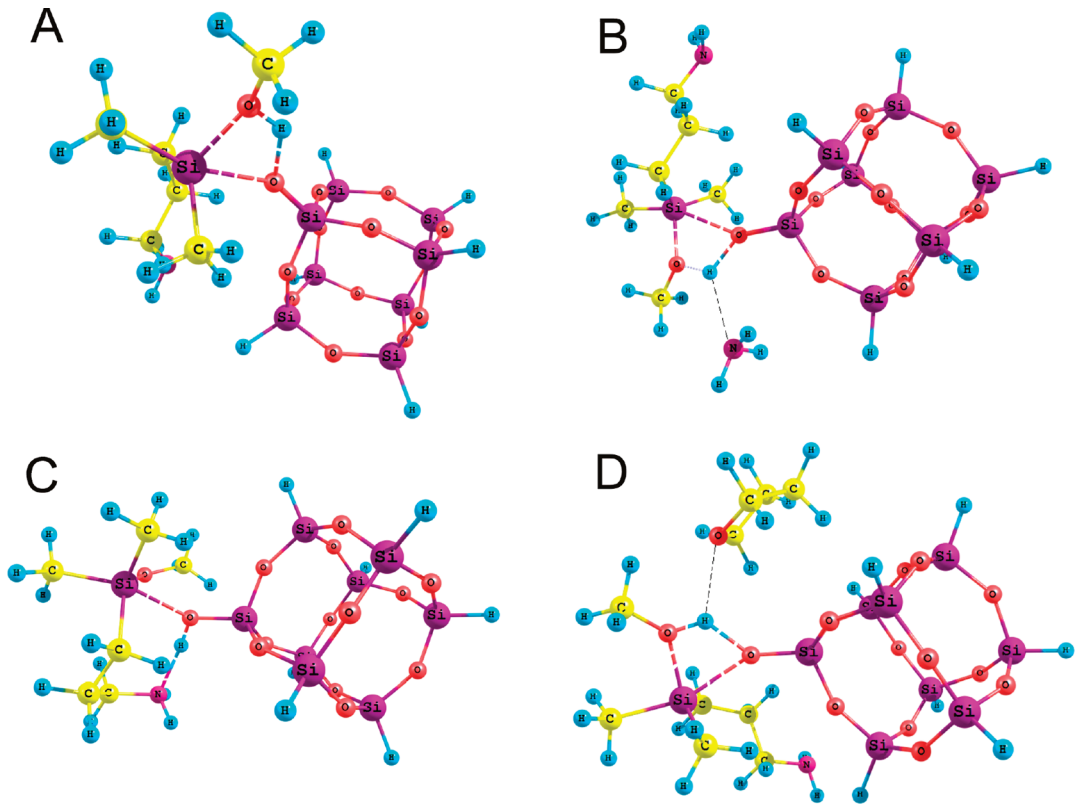


**Figure 6.** (A) TS of noncatalytic and catalytic reactions with (B) $NH_3$ used instead of the second APDMS molecule, (C) of the intracatalytic reaction, and (D) with THF as a catalyst of reaction between silsesquioxane silanol and APDMS.

**TABLE 3: Calculated Activation Energy ($E^{\neq}$ or $G^{\neq}$) of Non-, Intra-, and Intercatalytic Reactions between APDMS and Silsesquioxane in Different Media Using the SM5.42R (GAMESOL 3.1) and IEFPCM (Gaussian 03) Methods with Geometry Determined with the HF/6-31G(d,p) Basis Set**

| reaction type | solvent | method | total energy ($E$ or $G$) (Hartree) | $E^{\neq}$ or $G^{\neq}$ (kJ/mol) |
|---|---|---|---|---|
| noncatalytic | | HF/6-31G(d,p) | −3945.99399662 | 146 |
| noncatalytic | | B3LYP/6-31G(d,p) | −3958.32331637 | 117 |
| intracatalytic | | HF/6-31G(d,p) | −3945.97613166 | 193 |
| intracatalytic | | B3LYP/6-31G(d,p) | −3958.32008557 | 125 |
| intercatalytic ($NH_3$) | | HF/6-31G(d,p) | −4002.18734568 | 152 |
| intercatalytic ($NH_3$) | | B3LYP/6-31G(d,p) | −4014.88656981 | 102 |
| intercatalytic (THF) | | HF/6-31G(d,p) | −4176.99354366 | 117 |
| intercatalytic (THF) | | B3LYP/6-31G(d,p) | −4190.80514508 | 60 |
| noncatalytic | THF | SM5.42R/6-31G(d) | −3945.91229270 | 116 |
| noncatalytic | THF | IEFPCM/B3LYP/6-31G(d) | −3958.33420486 | 88 |
| noncatalytic | hexane | SM5.42R/6-31G(d) | −3945.90604424 | 142 |
| noncatalytic | heptane | IEFPCM/B3LYP/6-31G(d) | −3958.32790848 | 102 |
| noncatalytic | water | SM5.42R/6-31G(d) | −3945.914622763 | 146 |
| intercatalytic ($NH_3$) | THF | SM5.42R/6-31G(d) | −4002.094475578 | 128 |
| intercatalytic (THF) | THF | SM5.42R/6-31G(d) | −4176.892885257 | 117 |
| intercatalytic (THF) | THF | IEFPCM/B3LYP/6-31G(d) | −4190.80327655 | 96 |
| intercatalytic ($NH_3$) | hexane | SM5.42R/6-31G(d) | −4002.088416607 | 153 |
| intercatalytic ($NH_3$) | heptane | IEFPCM/B3LYP/6-31G(d) | −4014.89165119 | 91 |
| intercatalytic ($NH_3$) | THF | IEFPCM/B3LYP/6-31G(d) | −4014.89889880 | 108 |
| intercatalytic ($NH_3$) | water | SM5.42R/6-31G(d) | −4002.099041861 | 166 |
| intracatalytic | THF | SM5.42R/6-31G(d) | −3945.874866118 | 215 |
| intracatalytic | THF | IEFPCM/B3LYP/6-31G(d) | −3958.33324560 | 117 |
| intracatalytic | hexane | SM5.42R/6-31G(d) | −3945.878914400 | 214 |
| intracatalytic | heptane | IEFPCM/B3LYP/6-31G(d) | −3958.32533286 | 109 |

Prior to discussing the role of solvation effects on the energetics of reaction, merits of the intra- versus interautocatalytic reaction mechanisms are explored. Calculations of the transition state for the intracatalytic reaction show that the $G^{\neq}$ value calculated with consideration for solvation effects, as well as the $E^{\neq}$ value in vacuum, are consistently higher than the intercatalytic reaction (Table 3). In addition, $H^+$ transfer is facilitated when both the methoxy oxygen in the leaving group, and N from the catalyst, are on the same side of the silanol. However, this geometry could not be achieved (compare structures in Figure 6B,C); thus, the intracatalytic mechanism is considered not viable.

The APDMS/silsesquioxane reaction kinetics is significantly different in hexane and THF solvents. In general, the presence of oxygen in THF leads to a higher polarity of THF (dielectric constant $\varepsilon = 7.52$ compared to hexane $\varepsilon = 1.89$, at 20 °C).

This affords the possibility for THF to form hydrogen bonds with both silsesquioxane silanols and amino groups of APDMS. Therefore, THF can compete with APDMS molecules to form hydrogen bonds with silanols decreasing the lifetime of prereaction complexes. For instance, changes in Gibbs free energy from hydrogen bond formation of $RN(H_2)\cdots H-OSi\equiv$, $SiO(CH_3)\cdots H-OSi\equiv$, and $(CH_2)_4O\cdots H-OSi\equiv$ in THF are $\Delta G = -43.9$, $-28.7$, and $-26.2$ kJ/mol (SM5.42R/6-31G(d)//6-31G(d,p)), respectively. This shows that the energy of the bond between the methoxy oxygen of APDMS or the THF oxygen, with the silsesquioxane silanol, $O\cdots H-OSi\equiv$, is very similar. On the other hand, since the transition state of the APDMS/silsesquioxane reaction involves a $H^+$ transfer as the limiting stage, the TS is more polar than prereaction complexes. Polar solvents like THF more strongly stabilize the TS and reduce the free activation energy. For example the free energy of solvation is $\Delta G_s = -76.7$ kJ/mol (IEFPCM/B3LYP/6-31G(d,p)//6-31G(d,p)), compared with the sum of $\Delta G_s$ for reactants ($\Sigma\Delta G_s = -22.2$ kJ/mol) for the $NH_3$ intercatalytic reaction. Thus, there are several opposing solvation factors that affect the APDMS/silsesquioxane reaction rate. Therefore, the prereaction complexes and TS of noncatalytic and intercatalytic ($NH_3$ and THF) reactions were calculated taking into account solvation effects of hexane (or heptane) and THF.

Results of prereaction complex studies with SM5.42R/6-31G(d)//6-31G(d,p) calculations show that changes in the Gibbs free energy are more negative (by 5 and 10 kJ/mol) in hexane than in THF ($\Delta G_{hexane(THF)} = G_{complex} - G_{APDMS} - G_{SS}$ and $\Delta\Delta G_{HT} = \Delta G_{hexane} - \Delta G_{THF} < 0$), despite a larger negative Gibbs free energy of solvation ($\Delta G_s$) in THF (as a more polar solvent) than hexane ($\Delta G_{s,THF} - \Delta G_{s,hexane} \approx -10$ kJ/mol). As a whole, an increase in the solvent polarity (hexane < THF < water) leads to a larger negative Gibbs free energy of solvation (not shown here); however, changes in the total $G$ values show the opposite trend due to desolvation effects occurring from the formation of complexes with overlapping solvate shells of interacting molecules. Thus the lifetime of prereaction complexes is one to 2 orders of magnitude longer in hexane than in THF solution.

Transition-state calculations with SM5.42R/6-31G(d)//6-31G(d,p) show that the activation Gibbs free energy ($G^{\neq} = G_{TS} - \Sigma G_{reactants}$) for the noncatalytic reaction in hexane (142 kJ/mol) is larger than in THF (116 kJ/mol) but lower than in water (146.0 kJ/mol). These relatively large $G^{\neq}$ values illustrate the importance of catalytic effects in these reactions. According to IEFPCM/B3LYP/6-31G(d,p) calculations, $G^{\neq} = 102$ kJ/mol for the noncatalytic reaction in heptane, for the $NH_3$ intercatalytic reaction $G^{\neq}$ is found to be 91 kJ/mol. Although the intercatalytic $G^{\neq}$ is lower, all of these values are significantly larger than the first moment of the $f(E)$ distribution, as well as the apparent activation energy (Figure 5). This discrepancy will be addressed shortly.

For the noncatalytic reaction, the $G^{\neq}$ value (IEFPCM/B3LYP/6-31G(d,p)) is lower for the process in THF than in heptane (hexane) but the opposite result is found for the intercatalytic reaction (Table 3). These results are in agreement with the experimental data showing a higher reactivity in hexane than THF, because of the difference in the effects of hexane and THF solvents on $H^+$ transfer in the intercatalytic reaction. The intercatalytic reactions in THF catalyzed by $NH_3$ are characterized by a larger $G^{\neq}$ value than that catalyzed by THF. This result is due to the dragging of a catalyst molecule following $H^+$ transfer[34] because the search of the TS was performed using a nondynamic approach.

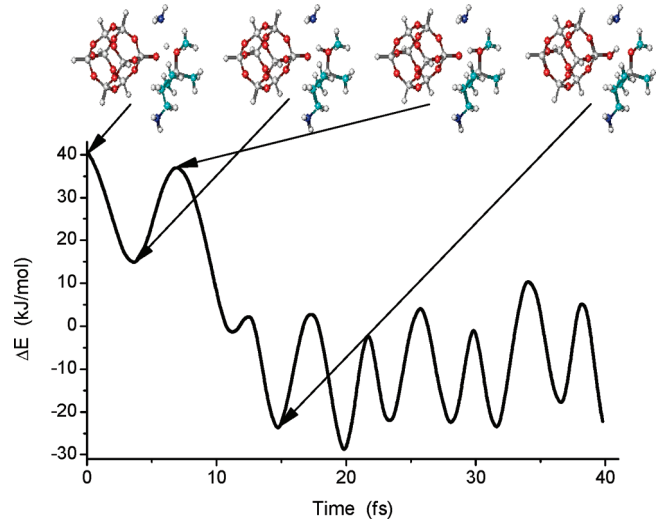


**Figure 7.** Changes in the total energy obtained from calculations using the dynamic reaction coordinate (DRC, basis set 6-31G(d,p)) method from the TS for catalytic reaction as a starting point (the geometry corresponding to $t = 14.6$ fs is close to the geometry of the prereaction complex).

The dynamic reaction coordinate (DRC) calculations for the autocatalytic APDMS/silsesquioxane reaction (Figure 7) show that a significant portion of required energy for the system in the TS is spent on $H^+$ transfer. The initial point of the DRC curve corresponds to the autocatalytic reaction transition state (Figure 6b). The first minimum corresponds to attachment of $H^+$ to $O_{APDMS}$ (motion toward products), but then the $H^+$ moves toward O from the silsesquioxane silanol (motion toward reactants), over a barrier (with maximum corresponding to the third structure in Figure 7) toward a minimum (the fourth structure). The amount of time required for all these motions to occur is ~14 fs. This is sufficient time for the O−H stretching vibration in a strongly disturbed silanol (~2400 $cm^{-1}$). The imaginary frequency calculated in the TS is 1493 $cm^{-1}$, corresponding to $H^+$ transfer. Thus, the largest contribution to total energy change in the TS, transforming the DRC calculations toward reactants, are relatively fast because they are related to $H^+$ motion. This energy (~60 kJ/mol) is much smaller than the activation energy calculated using a nondynamic search of the TS without solvent (Table 3) because displacements of other atoms such as O, C, N, and Si in APDMS and silsesquioxane are much smaller than $H^+$ during this time. Thus $H^+$ transfer is the limiting stage of the APDMS/silsesquioxane reaction. The main role of the catalyst (e.g., the second APDMS molecule or the amino group of the APDMS reactant) is weakening of the SiO−H bond in the silsesquioxane silanol (up to tunneling $H^+$ transfer to the N atom). This promotes $H^+$ transfer to the O atom of the APDMS reactant, leading to a weakening of the $Si-OCH_3$ bond in APDMS, and elimination to form $CH_3OH$. The SiOSi bond formation between APDMS and silsesquioxane occurs simultaneously with $Si-OCH_3$ bond breaking in APDMS. Since the lifetime of the prereaction complexes is larger in hexane than in THF (SM5.42R/6-31G(d)//6-31G(d,p)), the reaction rate in the former is greater.

## Conclusions

The APDMS/silsesquioxane reaction and APDMS silica reaction occur much faster in hexane than in THF. In hexane the apparent rate constant is maximum at 245 K, above which the reaction slows due to a reduction in prereaction complex formation

and below which the reaction slows due to the normal reason of insufficient energy to overcome the activation barrier. The stronger competitive effects of the polar THF solvent on the formation of prereaction complexes, due to hydrogen bonding of THF to silsesquioxane molecules in part explains the solvent effect on reaction rate. The experimental data and computational results suggest that the autocatalytic reaction is second-order with respect to APDMS, a second APDMS molecule plays the role of catalyst. The DRC calculations show that the major portion of the activation energy is spent on $H^+$ transfer, which occurs in approximately 15 fs. During this time the displacements of other atoms from APDMS and silsesquioxane are insignificant. The estimation of the activation energy using the DRC method gives better results than nondynamic calculations.

**Acknowledgment.** This work was supported in part by a grant from the Petroleum Research Fund administered by the American Chemical Society. V.M.G. thanks the STCU (Ukraine) for financial support (grant no 4481).

## References and Notes

(1) Pluedeman, E. P. In *Silane Coupling Agents*; Plenum Press: New York and London, 1991.

(2) Wilson, R; Spiller, D. G.; Prior, Ian, A.; Veltkamp, K.; Hutchison, J. A. *ACS Nano* **2007**, *1*, 487–493.

(3) Schena, M. In *Microarray Biochip Technology*; Eaton Publishing: Natick, MA, 2000.

(4) Moon, J. H.; McDaniel, W.; Hancock, L. F. *J. Colloid Interface Sci.* **2006**, *300*, 117–122.

(5) Blitz, I. P.; Blitz, J. P.; Gun'ko, V. M.; Sheeran, D. J. *Colloids Surf., A* **2007**, *307*, 83–92.

(6) Jal, P. K.; Patel, S.; Mishra, B. K. *Talanta* **2004**, *62*, 1005–1028.

(7) Lai, C.-Y.; Trewyn, B. G.; Jeftinja, D. M.; Jeftinja, K.; Yu, S; Jeftinja, S.; Lin, Victor S.-Y. *J. Am. Chem. Soc.* **2003**, *125*, 4451–4459.

(8) Shunai, C.; Zheng, L; Ohsuna, T.; Sakamoto, K.; Teraski, O.; Tatsumi, T. *Nature* **2004**, *429*, 281–284.

(9) Vansant, E. F.; Van der Voort, P.; Vrancken, K. C. In *Characterization and Chemical Modification of the Silica Surface*; Elsevier: Amsterdam, 1991, pp 194−209.

(10) Kaas, R. L.; Kardos, J. L. *Polym. Eng. Sci.* **1971**, *11*, 11–18.

(11) Blitz, J. P.; Murthy, R. S. S.; Leyden, D. E. *J. Am. Chem. Soc.* **1987**, *109*, 7141–7145.

(12) Blitz, J. P.; Murthy, R. S. S.; Leyden, D. E. *J. Colloid Interface Sci.* **1988**, *126*, 387–392.

(13) Tripp, C. P.; Hair, M. L. *J. Phys. Chem.* **1993**, *97*, 5693–5698.

(14) Tripp, C. P.; Hair, M. L. *Langmuir* **1996**, *12*, 6407–6409.

(15) White, L. D.; Tripp, C. P. *J. Colloid Interface Sci.* **2000**, *227*, 237–243.

(16) White, L. D.; Tripp, C. P. *J. Colloid Interface Sci.* **2000**, *232*, 400–407.

(17) Frei, R.; Blitz, J. P. *J. Undergrad. Chem. Research* **2008**, *7*, 1–5.

(18) Yoshino, A.; Okabayashi, H.; Shimizu, I.; O'Connor, C. J. *Colloid Polym. Sci.* **1997**, *275*, 672–680.

(19) Shimizu, I.; Yoshino, A.; Okabayashi, H.; Hirofumi, N.; Nishio, E.; O'Connor, C. J. *J. Chem. Soc. Faraday Trans.* **1997**, *93*, 1971–1979.

(20) Gun'ko, V. M.; Vedamuthu, M. S.; Henderson, G. L.; Blitz, J. P. *J. Colloid Interface Sci.* **2000**, *228*, 157–170.

(21) Vedamuthu, M. S.; Painter, S.; Ancheta, J.; Blitz, J. P. *J. Undergrad Chem. Research* **2002**, *1*, 5–9.

(22) Blanc, F.; Chabanas, M.; Coperet, C.; Frenet, B.; Herdweck, E. *J. Organomet. Chem.* **2005**, *690*, 5014–5026.

(23) Cho, H. M.; Weissman, H.; Wilson, S. R.; Moore, J. S. *J. Am. Chem. Soc.* **2006**, *128*, 14742–14743.

(24) Djikstra, T. W.; Duchateau, R.; van Santen, R. A.; Meetsma, A.; Yap, G. P. A. *J. Am. Chem. Soc.* **2002**, *124*, 1931–1936.

(25) Feher, F. J.; Newman, D. A. *J. Am. Chem. Soc.* **1990**, *112*, 1931–1936.

(26) Frisch, M. J.; Trucks, G. W.; Schlegel, H. B.; Scuseria, G. E.; Robb, M. A.; Cheeseman, J. R.; Zakrzewski, V. G.; Montgomery, J. A., Jr.; Stratmann, R. E.; Burant, J. C.; Dapprich, S.; Millam, J. M.; Daniels, A. D.; Kudin, K. N.; Strain, M. C.; Farkas, O.; Tomasi, J.; Barone, V.; Cossi, M.; Cammi, R.; Mennucci, B.; Pomelli, C.; Adamo, C.; Clifford, S.; Ochterski, J.; Petersson, G. A.; Ayala, P. Y.; Cui, Q.; Morokuma, K.; Malick, D. K.; Rabuck, A. D.; Raghavachari, K.; Foresman, J. B.; Cioslowski, J.; Ortiz, J. V.; Baboul, A. G.; Stefanov, B. B.; Liu, G.; Liashenko, A.; Piskorz, P.; Komaromi, I.; Gomperts, R.; Martin, R. L.; Fox, D. J.; Keith, T.; Al-Laham, M. A.; Peng, C. Y.; Nanayakkara, A.; Gonzalez, C.; Challacombe, M.; Gill, P. M. W.; Johnson, B. G.; Chen, W.; Wong, M. W.; Andres, J. L.; Head-Gordon, M.; Replogle, E. S.; Pople, J. A. *Gaussian 98*, revision A.11.2 Gaussian, Inc.: Pittsburgh, PA, 1998.

(27) Frisch, M. J.; Trucks, G. W.; Schlegel, H. B.; Scuseria, G. E.; Robb, M. A.; Cheeseman, J. R.; Montgomery, J. A., Jr.; Vreven, T.; Kudin, K. N.; Burant, J. C.; Millam, J. M.; Iyengar, S. S.; Tomasi, J.; Barone, V.; Mennucci, B.; Cossi, M.; Scalmani, G.; Rega, N.; Petersson, G. A.; Nakatsuji, H.; Hada, M.; Ehara, M.; Toyota, K.; Fukuda, R.; Hasegawa, J.; Ishida, M.; Nakajima, T.; Honda, Y.; Kitao, O.; Nakai, H.; Klene, M.; Li, X.; Knox, J. E.; Hratchian, H. P.; Cross, J. B.; Adamo, C.; Jaramillo, J.; Gomperts, R.; Stratmann, R. E.; Yazyev, O.; Austin, A. J.; Cammi, R.; Pomelli, C.; Ochterski, J. W.; Ayala, P. Y.; Morokuma, K.; Voth, G. A.; Salvador, P.; Dannenberg, J. J.; Zakrzewski, V. G.; Dapprich, S.; Daniels, A. D.; Strain, M. C.; Farkas, O.; Malick, D. K.; Rabuck, A. D.; Raghavachari, K.; Foresman, J. B.; Ortiz, J. V.; Cui, Q.; Baboul, A. G.; Clifford, S.; Cioslowski, J.; Stefanov, B. B.; Liu, G.; Liashenko, A.; Piskorz, P.; Komaromi, I.; Martin, R. L.; Fox, D. J.; Keith, T.; Al-Laham, M. A.; Peng, C. Y.; Nanayakkara, A.; Challacombe, M.; Gill, P. M. W.; Johnson, B.; Chen, W.; Wong, M. W.; Gonzalez, C.; Pople, J. A. *Gaussian 03 Revision D.01 and E.01*; Gaussian, Inc.: Wallingford, CT, 2003.

(28) (a) Schmidt, M. W.; Baldridge, K. K.; Boatz, J. A.; Elbert, S. T.; Gordon, M. S.; Jensen, J. J.; Koseki, S.; Matsunaga, N.; Nguyen, K. A.; Su, S.; Windus, T. L.; Dupuis, M.; Montgomery, J. A. *J. Comput. Chem.* **1993**, *14*, 1347. (b) Granovsky, A. A. www.http://classic.chem.msu.su/gran/gamess/index.html.

(29) Xidos, J. D.; Li, J.; Zhu, T.; Hawkins, G. D.; Thompson, J. D.; Chuang, Y.-Y.; Fast, P. L.; Liotard, D. A.; Rinaldi, D.; Cramer, C. J.; Truhlar, D. G. *GAMESOL*, version 3.1; University of Minnesota: Minneapolis, 2002.

(30) Atkins, P. W. In *Physical Chemistry*, 6th ed., Oxford University Press: Oxford, UK, 1998.

(31) Trens, P.; Denoyel, H. *Langmuir* **1996**, *12*, 2781–2784.

(32) Bogart, G. R.; Leyden, D. E. *J. Colloid Interface Sci.* **1994**, *167*, 27–34.

(33) Provencher, S. W. *Comput. Phys. Commun.* **1982**, *27*, 213–227.

(34) Gun'ko, V. M.; Voronin, E. F.; Pakhlov, E. M.; Chuiko, A. A. *Langmuir* **1993**, *9*, 716–722.

JP9002998